Unsteady Cavitation at the Tongue of the Volute of a Centrifugal Pump

Rudolf Bachert[1,2]
AUMA Riester GmbH & Co. KG,
Aumastrasse 1,
79379 Muellheim, Germany
e-mail: rudolf.bachert@auma.com

Bernd Stoffel
Former Head
Laboratory for Turbomachinery and Fluid Power,
Darmstadt University of Technology,
Magdalenenstrasse 4,
64289 Darmstadt, Germany
e-mail: bernd.stoffel@fst.tu-darmstadt.de

Matevž Dular[2]
Laboratory for Water and Turbine Machines,
University of Ljubljana,
Askerceva 6,
1000 Ljubljana, Slovenia
e-mail: matevz.dular@fs.uni-lj.si

The paper deals with unsteady effects of cavitation at the tongue of the volute of a centrifugal pump. For the investigations parts of the volute casing, including the tongue and the hub of the impeller, were made of acrylic glass. Experiments were carried out at a flow rate above optimal value (slight overload) and at 3% head drop conditions. In this operating point there was no cavitation present in the impeller of the pump, hence, the whole 3% head drop resulted from cavitation on the tongue of the volute. By use of particle image velocimetry combined with special fluorescent particles it was possible to obtain information about the velocity field outside and inside the cavitating zone. An additional camera provided information about the location and extent of cavitation. The results imply that cloud cavitation similar to the one seen on single hydrofoils appears on the tongue. Periodical evolution of cavitation structures, from incipient to developed, with cavitation cloud shedding, is seen during each passing of a blade. The Results imply that greater consideration should be given to the possibility of cavitation appearance on the tongue of the volute as it is possible that this cavitation location alone causes the 3% head drop. Moreover, the appearance of unsteady cavitation in a higher-pressure region, such as the volute of the pump, can cause severe erosion to the solid surfaces.
[DOI: 10.1115/1.4001570]

Keywords: cavitation, particle image velocimetry, centrifugal pump, tongue, volute

1 Introduction

To avoid or to reduce the effects of cavitation by design and operation measures, there is a persistent need of improving the detailed understanding of the physical phenomena underlying its harmful effects. It is well known that flow separation often occurs in the spiral casing of centrifugal pumps, particularly in the vicinity of the tongue, when they are operating at off design conditions, i.e., flow rates lower or higher than the optimal [1]. Flow separation, characterized by unsteady shedding of vortices from the tongue, can also be an important source of vibration and noise [2]. The other type of instability, common to hydraulic turbomachines, is cavitation, where the pressure locally drops to and below the vapor pressure of the liquid. Occurrence of cavitation in hydraulic machines leads to problems such as shock waves, noise, and dynamic effects that lead to decreased equipment performance and, frequently to equipment failure [3]. In the case of centrifugal pumps, large attached cavities preferably form on the suction surfaces of the blades near their leading edge [1].

The present study deals with a special case of separated flow in a pump operating at overload conditions, where cavitation at the tongue of the volute casing occurs prior to the cavitation on the blades. In this case the standard threshold level of 3% head drop [4] due to cavitation does not come from cavitation in the impeller but from the cavitation on the tongue of the volute. Three reasons that have not yet been thoroughly investigated are probably responsible for this phenomenon.

1. The pressure rise generated by the impeller decreases more and more with an increase in flow rate (see Fig. 5). This means that the static pressure in the vicinity of the tongue at overload conditions is lower, making the system more prone to cavitation.
2. At specific flow rates q ($q=Q/Q_{opt}$) bigger than optimal ($q>1$), the direction of the absolute velocity at the blade trailing edge deviates from the angle of zero incidence of the tongue shape. This leads to an incidence angle, which increases with increasing flow rate. Because the flow angle is mostly larger than the angle of zero incidence of the tongue, the stagnation point shifts from the leading edge of the tongue to a location on the tongue side oriented toward the impeller (inner side). A low pressure zone develops on the opposite side, which is oriented toward the volute discharge and cavitation forms (Fig. 1).
3. In addition, the passing blades of the impeller create a periodically varying velocity and pressure field in the vicinity of the tongue. This unsteady flow field is prone to cavitation and has a distinct effect on various cavitation phenomena at the tongue. For example, it is well known that unsteady cavitation is the most erosive type of cavitation [5], hence, it is not surprising that often local erosion damage is found at the tongue of centrifugal pumps after they have been operated at overload conditions for elongated periods of time [1].

The investigations of velocity field in the vicinity of or inside cavitation is a complex task. Different investigations with the aid of probe measurements were performed in the past [6]. With this method the velocity can be measured only in one point at a time, hence, only an average velocity field can be determined. The problem can be solved by particle image velocimetry (PIV) as first showed by Zhang et al. [7]. They employed PIV to examine the turbulent flow in the wake of an open partial cavity. Laberteaux and Ceccio [8] measured velocities in developed cavitating flow with vapor cloud separation. However, they were unable to obtain the information about velocity field inside the cavitation itself. The problem they faced was overexposure of the particles added to the water (they were not visible since the vapor structure re-

[1]Corresponding author.
[2]Previous address: Laboratory for Turbomachinery and Fluid Power, Darmstadt University of Technology, Magdalenenstr. 4, 64289 Darmstadt, Germany.

Contributed by the Fluids Engineering Division of ASME for publication in the JOURNAL OF FLUIDS ENGINEERING. Manuscript received October 15, 2009; final manuscript received March 23, 2010; published online May 19, 2010. Assoc. Editor: Olivier Coutier-Delgosha.

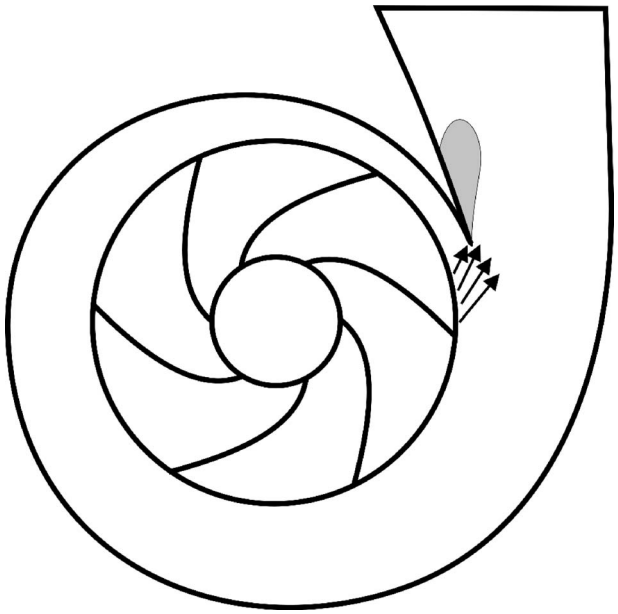

Fig. 1 Schematic representation of the flow field in the vicinity of the volute tongue

flects much more light) so the velocity field inside the cavitation structure could not be measured. Recently, a promising method based on X-ray absorption and phase-contrast enhancement, where the velocity of both liquid and vapor phase could be measured, was introduced by Vabre et al. [9]. The method applied in the present study, which allows flow velocity measurements outside and also inside the vapor structure is a combination of PIV and fluorescent particles. The technique was already successfully applied to simpler geometries such as hydrofoils [10,11].

During the experiment, the pump was operating at overload flow rate and cavitation condition leading to 3% head drop. Visual access to the whole flow field enabled confirmation that no cavitation is present within the impeller. Also, detailed observations of the cavitation structures on the tongue of the volute casing were made.

The main aim of the study was to measure the velocity field in the vicinity of the tongue of the volute casing to check the hypothesis of the high angle of attack on the tongue of the spiral casing and the unsteady flow conditions in the region. For this purpose, PIV was applied at the tongue of a centrifugal pump.

Results show that the velocity direction at the blade trailing edge indeed deviates from the angle of zero incidence of the tongue shape, oscillates significantly and that this indeed causes appearance of cavitation on the tongue that results in the 3% head drop of the pump.

2 Experimental Set-Up

Experiments were set up in a cavitation tunnel at the Laboratory for Turbomachinery and Fluid Power in the Darmstadt University of Technology.

2.1 The Pump and the Test Rig. The radial impeller of the test pump (Fig. 2) has a three-dimensional blade geometry typical for standard centrifugal pumps produced by pump manufacturers. It has six blades, an outer diameter of 260 mm, and the specific speed is $n_s = 26\ \text{min}^{-1}$.

$$n_s = \frac{\omega\sqrt{Q}}{\sqrt[4]{h^3}} \tag{1}$$

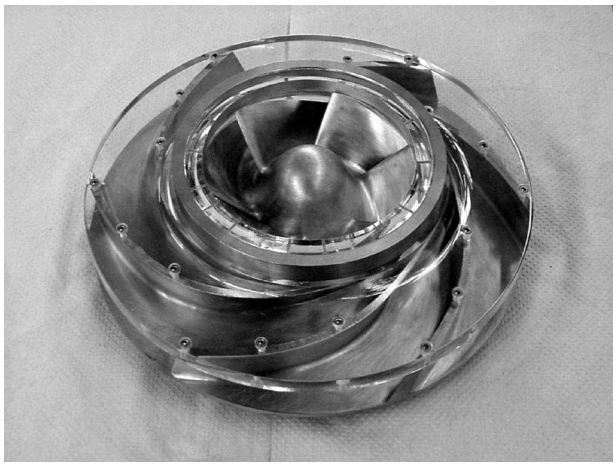

Fig. 2 Impeller of the test pump with transparent front shroud

where ω (in min^{-1}) is the rotational frequency, Q (in m^3/s) is the flow rate at best efficiency point and, h is the corresponding head (in m).

The rotational frequency of the impeller was 2000 min^{-1} during the experiments for which the volume flow rate Q at the best efficiency point ($Q = Q_{opt}$; $q = 1.0$) is 143 m^3/h. To provide optical access to the impeller blades, the front shroud of the impeller was made of acrylic glass. Experiments were performed at overload conditions at $q = 1.17$, where the value of net positive suction head (NPSH) was held constant at $\text{NPSH} = \text{NPSH}_{3\%} = 4$ m.

$$\text{NPSH} = \frac{p_i - p_v}{\rho \cdot g} + \frac{c_i^2}{2g} \tag{2}$$

where p_i is the static pressure at pump inlet, p_v is the vapor pressure, and c_i is the absolute velocity at pump inlet.

In Fig. 3, the cross-section through the pump is shown. The suction nozzle, the suction sided cover plate of the casing and the volute with the tongue were made of transparent acrylic glass. This enabled optical access to the outlet of the impeller to the tongue and to the volute discharge in the axial direction. This was also the direction for the digital camera sight, which was used for the velocity measurements. The laser light sheet is brought in perpendicularly to the axis of rotation through a window in the outer casing wall.

The closed test loop used for the investigations on the test pump is shown in Fig. 4. The test rig and the test pump are

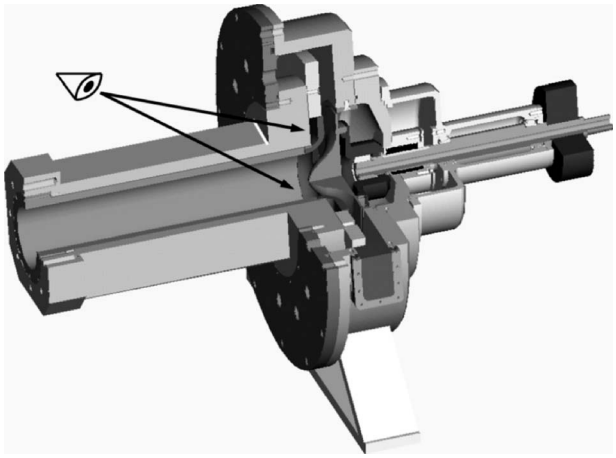

Fig. 3 Cross-section through the pump installation with noted view point of cameras

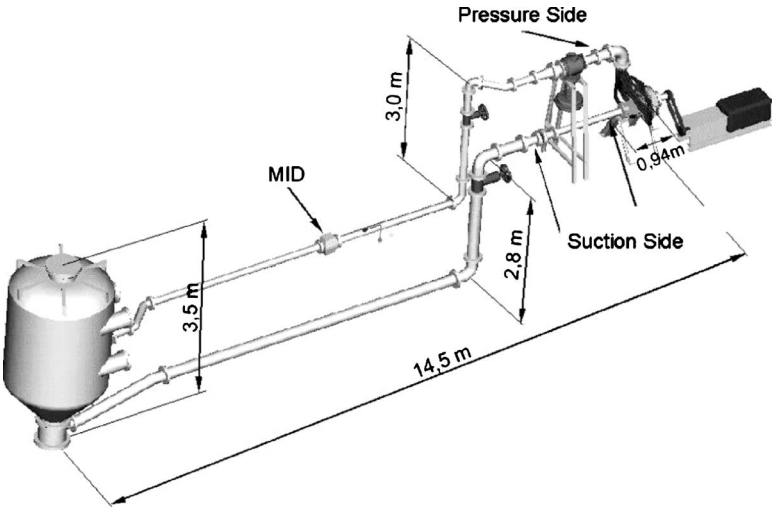

Fig. 4 Test loop for pump tests

equipped with the necessary instrumentation to determine the operating conditions (rotational frequency n, shaft torque T, flow rate Q, and pressures at the pump inlet and outlet p_{s1} and p_{s2}) of the test pump.

The flow rate was measured with an inductive flow meter Fischer and Porter type D10D, DN 150 with an uncertainty of ± 3.5 m^3/h. The system pressures p_{s1} and p_{s2} were measured with sensors JPB-type 304 at four pressure taps on the pipe and then averaged. The uncertainty of the measurements was ± 20 mbar. The fluid temperature was measured by Jumo PT100 sensor with the uncertainty of ± 1.2 K. The rotating frequency was determined by a proximity sensor mounted on the pump shaft. The torque on the shaft was measured with the SteigerMohilo 02FE with the uncertainty of ± 1 Nm. Considering the combination of inaccuracies of pressure, flow rate, rotation frequency, and temperature measurements, the pump operating condition could be determined within $\pm 1.7\%$ of the measured value with a confidence level of 95% [12].

The quality of the water was monitored by measuring the gas content by an apparatus based on the Van Slyke method with an uncertainty of 1%. The water used for the experiments was almost saturated with gasses (more than 50 mg of dissolved and undissolved gas per liter of water) so that the effects of the tensile strength of the water were reduced to the minimum possible level. This condition is necessary since the variations in water quality can greatly influence the cavitation behavior [13].

Integral characteristics of the pump (q-H diagram at NPSH $=NPSH_{3\%}=4$ m on the left and NPSH-H diagram at $q=1.17$ on the right) are show in Fig. 5. The operating point in which the experiments were performed is also indicated.

Figure 6 shows the intake of the pump during operation at overload conditions ($q=1.17$) and at $NPSH=NPSH_{3\%}=4$ m. The camera position for the image in Fig. 6 is schematically presented in Fig. 3. The intake and the cover plate of the casing are both made out of transparent acrylic glass but since they are perpendicular to each other the light is refracted. In the bottom of the image in Fig. 6, we see the suction eye of the impeller and in the upper part we see the outer part of the blades with the blade trailing edges. As already mentioned, almost no cavitation can be seen on the blades. Some bubbles are present but their origin is the cavitation in the gap between the housing and the impeller. So it can be concluded that no cavitation is present on the blades of the impeller at the investigated conditions of operation.

2.2 Velocity Measurements. For the velocity measurements, the region of interest extended over the tongue of the volute. The illumination was provided by a vertical laser light sheet (Nd-YAG-Laser) approximately 1 mm thick and perpendicular to the observation axis. The position of the light sheet was at half width of the tongue, 24 mm from the front acrylic glass wall. Special fluorescent tracer particles (PMMA-RhB-Partikel-G029, mean diameter of 10 μs with standard deviation of 0.25 μs) were added to the water. The particles receive light from the laser at a wavelength of 532 nm (green spectrum) and emit light at a wavelength of 590 nm (yellow spectrum). By fitting the CCD cameras with an appropriate light filter (that filters the visible light but lets the light in yellow spectrum trough) it is possible to get suitable images of the tracer particles for the PIV analysis. Since the camera records

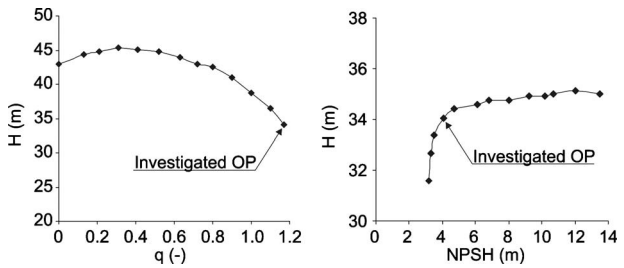

Fig. 5 Integral characteristics of the pump(q-H diagram at NPSH=4 m—left and NPSH-H diagram at q=1.17—right)

Fig. 6 View into the impeller at the investigated operating point (q=1.17, NPSH=4 m)

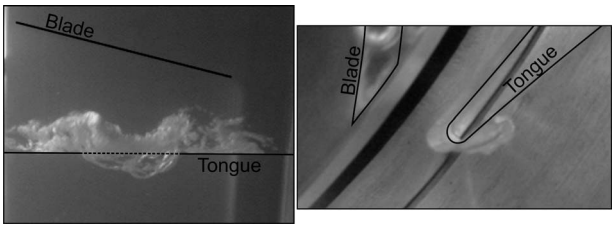

Fig. 7 Cavitation on the tongue of the volute (front view—left and side view—right)

only the light in the yellow spectrum, the cavitation structure is filtered out of that image and tracer particles inside it can also be detected. Despite less particles are detected inside the cavity a velocity field could be determined if the position of the light sheet was close enough to the front observation window (a more detailed description of the method can be found in previous paper by present authors [10]).

The camera and the laser shots with a duration of 10 ns were triggered by the control unit of the PIV-system. For the PIV analysis, two images with 30 μs time delay were recorded. Using the standard DANTEC DYNAMICSTUDIO software a cross correlation of the two images of tracer particles was made. The image size is 1280×860 pixels, corresponding to 85.9×57.7 mm^2 (6.7×10^{-2} mm/pixel). A low-pass Gaussian subpixel interpolation was used for the determination of the correlation peak. The size of the interrogation area was 16×16 pixels; the overlapping was 50% leading to distance of approximately 0.5 mm between the vectors. About 1% of the vectors in the region of interest were recognized as invalid "bad" vectors and were substituted. The dominant error in PIV measurements is usually the bias introduced by the subpixel peak finding algorithm. Taking all the uncertainties into consideration, we estimate a nominal particle image displacement error of about 0.1 pixels. Considering the variations of the velocity magnitudes (up to 30 m/s), i.e., particle image displacement (up to 1 mm or about 12 pixels), in the measured sections, the accuracy of the instantaneous velocity can be estimated to less than 1% [14].

2.3 Cavitation Image Capturing. Additionally to the PIV measurements another CCD camera (SensiCam with sensor CCD-Interline Progressive Scan) was used to capture images of cavitation in various parts of the pump. This gave a better perspective of the flow conditions in the system. Images were captured at 8 bit resolution. The size of captured image was 860×1280 pixels. The illumination was provided by a stroboscopic light triggered by the proximity sensor.

3 Results

3.1 Visualization. In Fig. 7, the cavitation at the tongue of the volute is shown.

The left image shows the view through the window in the casing radially inwards to the axis of rotation (this window was primarily installed for laser illumination for PIV measurements). In this image the movement of the impeller is from bottom to up. The leading edge of the tongue is located horizontally a bit below the middle of the image (marked by a black line in the image). At the moment when the image was taken, the blade trailing edge had just passed the tongue leading edge and is also visible through the transparent tongue (marked by a black line in the image). The right image shows the appearance of cavitation on the tongue from the side view (through the transparent front cover of the casing—the viewpoint, which was also used for the PIV measurements). Again, the blade trailing edge can be seen as it just passes the tongue leading edge.

The appearance of cavitation closely resembles that on a single hydrofoil in a cavitation tunnel [10]. The essential difference is

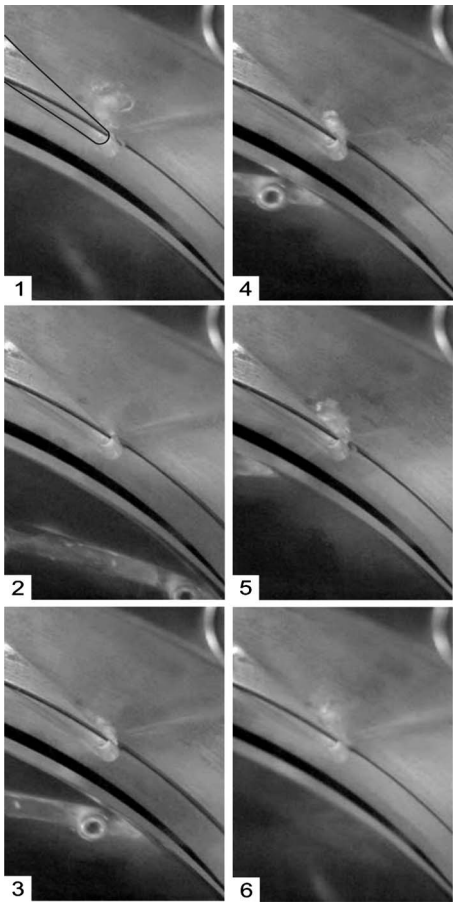

Fig. 8 A sequence showing evolution of the cavitation structure as the blade passes the tongue

that in the case of a single hydrofoil, the cavitation dynamics is dominated by periodical, self-excited cloud generation—the frequency of which is related to the flow velocity and the Strouhal number [15]. In the case of cavitation on a tongue of the pump, the pressure gradient from the suction side to the pressure side of the blade in combination with the wake of the blade instead cause the periodically varying of flow conditions at the tongue [2]. This results in periodical cavitation cloud generation with a frequency that corresponds to the blade passing frequency, which is illustrated in Fig. 8. The tongue was made out of transparent material and is hard to see in the images. Therefore, it is highlighted by a black line in the first image. The series of images shows one transition of the blade, where the whole cycle of the cavitation evolution can be seen.

In the first image the blade just moved out of the view of the camera. We can see a larger cavitation structure on the tongue, somewhat downstream of its leading edge. As will be shown later from the PIV results, the angle of incidence of the flow on the tongue is closest to optimal at this instant—no attached cavitation on the leading edge can be seen but a cloud generated at previous blade passing remains present.

Cavitation is barely visible in image No. 2. Actually only a separated cavitation cloud with relatively low volume fraction of vapor (hence, hardly visible) can be sensed further downstream of the leading edge of the tongue.

As the blade starts to approach the tongue the flow conditions become less and less optimal (image No. 3). A large attached cavitation structure grows on the leading edge of the tongue. Meanwhile the separated cloud has left the region of interest.

Image No. 4 shows the growth of the attached cavity while its separation from the tongue can be seen in image No. 5. The shape

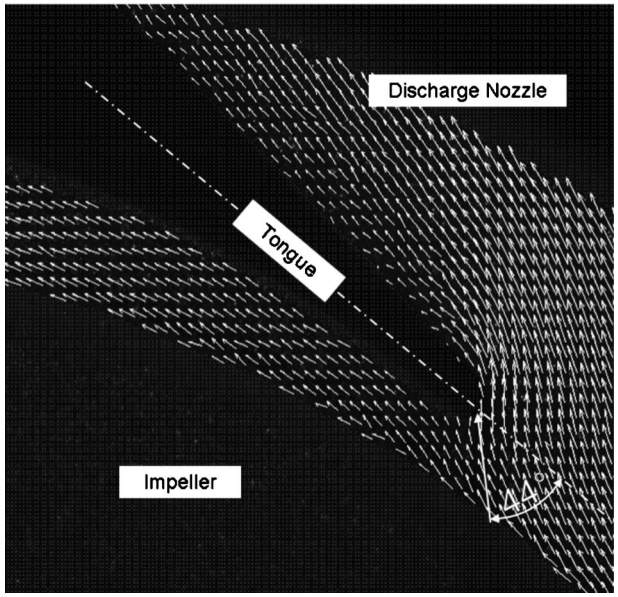

Fig. 9 Time averaged velocity field in the vicinity of the tongue with notated average incidence

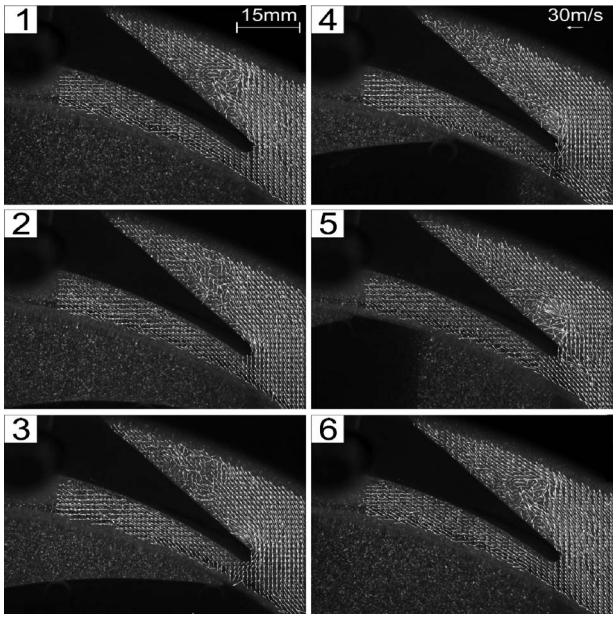

Fig. 10 A sequence showing the velocity field near the tongue as the impeller blade passes it

of the cavity closely resembles the one seen on single hydrofoils just before the cloud separation so it is fair to expect a reentrant jet formation at this point. The situation in image No. 6 is again the same as that of the first image, where the flow field around the leading edge of the tongue is more optimal, no attached cavitation is present and a larger vapor structure can be seen further downstream.

3.2 Velocity Measurements. The time averaged velocity field around the tongue of the spiral casing at $q=1.17$ and $NPSH_{3\%}$ is shown in Fig. 9. Such averaging obscures a large part of the information of the flow characteristics but we still get valuable data of the flow average conditions. The average field was determined from about 50 individual PIV images for the same operating point but for various angular positions of the impeller.

In a part of the area of the volute discharge (near to the upper right corner of the image), no velocity vectors are present. This is due to the obstruction of the laser light sheet by the casing.

As can be easily seen, the flow leaves the trailing edge of the impeller with a considerable radial velocity component, resulting in a high angle of incidence to the tongue of the spiral casing—the average incidence angle is about 44 deg. The location of the stagnation point shifts toward the bottom side of the tongue (oriented toward the impeller). On the opposite side of the tongue flow separation occurs, as it is known for overload operation points [2].

More interesting is the sequence, showing an unsteady velocity field around the tongue as the blade passes it (Fig. 10). The instances when the images were taken approximately correspond to the ones in Fig. 8.

In the first image the impeller blade has just left the region of interest (it is "downstream" of the tongue) and the successive blade has not entered yet (it is "upstream" of the tongue). The incidence angle on the tongue is a bit greater than 0 deg but the flow seems to be almost optimal. Correspondingly, the stagnation point is positioned near the center of the tongue leading edge. If we consider only the region in the vicinity of the leading edge we can see that the flow field seems to be undisturbed, hence, no or only marginal cavitation is present there. Further downstream a large separation zone exists. On the basis of past experience with PIV in cavitating flow [10,11] we can conclude that this corresponds to the separated cavitation cloud.

In image No. 2, the shadow from the blade trailing edge can hardly be seen in the lower right corner of the image. The flow now deviates significantly from the optimum. The stagnation point moves toward the inner contour of the tongue. The former large vapor cloud (characterized by highly disturbed flow) moves a bit downstream. Also a very small flow separation near the leading edge is present. This can be related to the growth of the attached part of the cavity.

The impeller blade is clearly visible in image No. 3. Its position coincides with the leading edge of the tongue. This is the case with worst flow conditions upstream of the tongue. The flow exiting the impeller is almost purely radial and the stagnation point moves even further to the inner contour of the tongue. The flow separation near the leading edge grows. Due to the poor data rate not many vectors were calculated in that region. Bachert [16] showed that low data rate in this region implies a dense bubble population characteristic for the attached type of cavitation. The separated cavitation cloud (large flow disturbance) that can be observed in the previous images is leaving the region of interest and is also getting smaller due to the transition into a higher-pressure region (cloud collapse is about to begin).

As the blade passes the leading edge of the tongue in image No. 4, the incidence angle has reached a maximum and starts to decrease, moving the stagnation point back toward the center of the tongue radius. The flow just downstream of the leading edge is more or less chaotic, implying that the flow field is influenced by a newly separated cavitation cloud. Meanwhile the cavitation cloud that resulted from the previous blade passage either has collapsed or moved downstream (out of the region of interest) with the flow.

Image No. 5 essentially shows a time extrapolation of image No. 4. The blade has moved on, enabling the fluid to approach the tongue at a more optimal direction (with relatively small angle of attack). The separated cavitation cloud grows and is convected downstream.

As the shedding is periodic with the blade passing frequency, image No. 6 corresponds to the situation shown in image No. 1.

In general it can be concluded that indeed the phenomenon of periodic cloud shedding on the tongue of the spiral casing is a result of the variation in velocity direction at impeller outlet.

To quantify the above results the incidence angle as a function of the blade trailing edge position is presented in Fig. 11. The diagram was derived by sequencing of about 50 PIV images. Φ is the angular position of the blade trailing edge –0 value represents

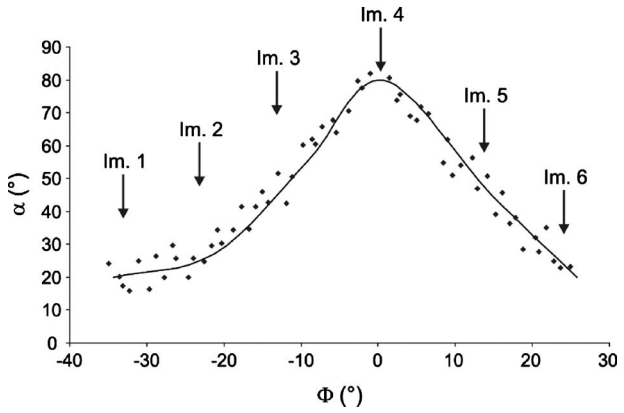

Fig. 11 Evolution of the incidence angle as a function of impeller blade position

a situation, where the trailing edge is positioned directly under the tongue leading edge. Approximate positions of the blade from Figs. 7 and 9 are indicated in the diagram.

It can clearly be seen very well that in the case of overload the incidence angle α does not fall below about 15 deg. As the blade approaches the tongue the flow starts to hit the tongue at a higher and higher angle, causing flow separation and consequently cavitation. The maximum angle of incidence is achieved approximately at the instant when the blade passes the leading edge of the tongue.

4 Conclusions

By means of direct visualization and PIV measurements we were able to explain the cause for the 3% head drop of a centrifugal pump operating at overload conditions. The study revealed that at overload conditions ($q=1.17$) and at $NPSH_{3\%}$ almost no cavitation is present on the blades of the impeller while the tongue of the spiral casing cavitates violently.

The cavitation phenomena at the tongue of the volute are similar to the cavitation on a single hydrofoil; however a distinctive difference in the source of unsteadiness exists. The cavitation on the single hydrofoil is induced by the reentrant jet formation at the cavity closure while in the case of the tongue of the volute, the unsteady cavitation cloud generation results from the unsteady flow field generated by the passing of the blades. A combination of the higher radial velocity component at the blade trailing edge on one hand and tongue designed for operation near optimal flow rate conditions on the other hand contribute to periodical generation of vapor clouds on the side of the tongue, which is oriented toward the volute discharge. Consequently, also the frequency of the vapor cloud shedding is the same as the blade passage frequency.

The study showed that careful consideration has to be given to the possibility of cavitation appearance on the tongue of the volute as it is possible that it alone causes the 3% head drop, which is considered as a limiting operation condition of a pump.

Acknowledgment

The authors R. Bachert and M. Dular would like thank the staff of the Laboratory for Turbomachinery and Fluid Power at Darmstadt University of Technology for the possibility to use the test rigs after their completion of Ph.D. studies.

Nomenclature

c_i = absolute velocity at pump intake
H = head
$NPSH_{3\%}$ = net positive suction head, where head drops for 3%
n_s = specific speed
p_i = pressure at pump intake
p_v = vapor pressure
Q = flow rate
Q_{opt} = optimal flow rate
q = specific flow rate
α = incidence angle
Φ = position of the blade
ρ = density
ω = rotating frequency

References

[1] Brennen, C. E., 1994, *Hydrodynamics of Pumps*, Concepts ETI, Inc., Norwich, VT and Oxford University Press, Oxford, UK.
[2] Chu, S., Dong, R., and Katz, J., 1993, "The Noise Characteristics Within the Volute of a Centrifugal Pump for Different Tongue Geometries," ASME Symposium on Flow Noise, Modelling, Measurement and Control, New Orleans, LA.
[3] Crowe, C. T., Elger, D. F., and Roberson, J. A., 2005, *Engineering Fluid Mecanics*, 8th ed., Wiley, New York.
[4] Gülich, J. F., 1999, *Kreiselpumpen*, Springer Verlag, Berlin, Heidelberg.
[5] Dular, M., Bachert, B., Stoffel, B., and Širok, B., 2004, "Relationship Between Cavitation Structures and Cavitation Damage," Wear, **257**(11), pp. 1176–1184.
[6] Stutz, B., and Reboud, J. L., 1997, "Experiment on Unsteady Cavitation," Exp. Fluids, **22**, pp. 191–198.
[7] Zhang, Y., Gopalan, S., and Katz, J., 1998, "On the Flow Structure and Turbulence in the Closure Region of Attached Cavitation," 22nd ONR Symposium on Naval Hydrodynamics, Washington, DC, pp. 227–238.
[8] Laberteaux, K. R., and Ceccio, S. L., 2001, "Partial Cavity Flows. Part 1. Cavities Forming on Models Without Spanwise Variation," J. Fluid Mech., **431**, pp. 1–41.
[9] Vabre, A., Gmar, M., Lazaro, D., Legoupil, S., Coutier, O., Dazin, A., Lee, W. K., and Fezzaa, K., 2009, "Synchrotron Ultra-Fast X-Ray Imaging of a Cavitating Flow in a Venturi Profile," Nucl. Instrum. Methods Phys. Res. A, **607**(1), pp. 215–217.
[10] Dular, M., Bachert, R., Stoffel, B., and Širok, B., 2005, "Experimental Evaluation of Numerical Simulation of Cavitating Flow Around Hydrofoil," Eur. J. Mech. B/Fluids, **24**(4), pp. 522–538.
[11] Dular, M., Bachert, R., Schaad, C., and Stoffel, B., 2007, "Investigation of a Re-Entrant Jet Reflection at an Inclined Cavity Closure Line," Eur. J. Mech. B/Fluids, **26**(5), pp. 688–705.
[12] Coleman, H. W., and Steele, W. G., 1999, *Experimentation and Uncertainty Analysis for Engineers*, 2nd ed., Wiley, New York.
[13] Iwai, Y., and Li, S., 2003, "Cavitation Erosion in Waters Having Different Surface Tensions," Wear, **254**, pp. 1–9.
[14] Yu, X. J., and Liua, B. J., 2007, "Stereoscopic PIV Measurement of Unsteady Flows in an Axial Compressor Stage," Exp. Therm. Fluid Sci., **31**(8), pp. 1049–1060.
[15] Dular, M., and Bachert, R., 2009, "The Issue of Strouhal Number Definition in Cavitating Flow," Journal of Mechanical Engineering, **55**(11), pp. 666–674.
[16] Bachert, R., 2004, "Dreidimensionale, instationäre Effekte kavitierender Strömungen—Analyse an Einzelprofilen und in einer Radialpumpe," Ph.D. thesis, Darmstadt University of Technology.